Pis'ma v ZhETF, vol. 95, iss. 6, pp. 355 – 360 © 2012 March 25

Phase diagram of superfluid ^{3}He in "nematically ordered" aerogel

R. Sh. Askhadullin[+], *V. V. Dmitriev*[1)], *D. A. Krasnikhin, P. N. Martynov*[+], *A. A. Osipov*[+], *A. A. Senin, A. N. Yudin*

Kapitza Institute for Physical Problems of the RAS, 119334 Moscow, Russia

[+]*Leypunsky Institute for Physics and Power Engineering, 249020 Obninsk, Russia*

Submitted 13 February 2012

Results of experiments with liquid ^{3}He immersed in a new type of aerogel are described. This aerogel consists of $Al_2O_3 \cdot H_2O$ strands which are nearly parallel to each other, so we call it as a "nematically ordered" aerogel. At all used pressures a superfluid transition was observed and a superfluid phase diagram was measured. Possible structures of the observed superfluid phases are discussed.

1. Introduction. An asymmetry of a volume filled by superfluid ^{3}He can influence on resulting pairing states. For example, in the case of a restricted geometry, boundaries of the container can suppress some components of the superfluid order parameter [1]. This distortion persists over a distance of the order of the temperature dependent superfluid correlation length $\xi = \xi(T)$, which diverges at the superfluid transition temperature. Theory predicts, that restricted geometry may stabilize superfluid phases which do not occur in bulk liquid ^{3}He [2, 3]. In superfluid ^{3}He inside a narrow gap (or in ^{3}He film) a planar type distortion is expected for the B phase in agreement with results of recent experiments [4, 5]. A spatially inhomogeneous order parameter with polar core may be realized in a narrow channel. This prediction has not been unambiguously confirmed by experiments, however measurements of mass supercurrent in narrow channels indicate a possible phase transition at the temperature just below the superfluid transition temperature [6, 7]. It is probable that these observations are associated with the transition into such kind of polar-type superfluid phase.

Another way to introduce the anisotropy into superfluid ^{3}He is to use ^{3}He confined in a globally anisotropic aerogel. It is known that the high porosity silica aerogel does not completely suppress the superfluidity of ^{3}He [8, 9]. It is also established that superfluid phases of ^{3}He in aerogel (A-like and B-like phases) are similar to superfluid phases of bulk ^{3}He (A- and B phases respectively) if the anisotropy of the aerogel is weak or if it corresponds to the squeezing deformation [10–14]. In this case the anisotropy of the aerogel influences only on the orientation of the ^{3}He superfluid order parameter and on its spatial structure [12, 13, 15]. However, recent theoretical investigations [16] show that the stretching anisotropy of the aerogel should result in a polar distortion of the A-like phase of superfluid ^{3}He in aerogel. Moreover, if the anisotropy is large enough then, in some range of temperatures just below the superfluid transition temperature, the pure polar phase may be more favorable than the A phase. Unfortunately silica aerogels are rather fragile, therefore in practice the stretching anisotropy can be obtained only in process of aerogel preparation [17] and the large value of this anisotropy is hardly achievable.

In this paper we present results of nuclear magnetic resonance (NMR) studies of liquid ^{3}He confined in a new type of aerogel [18]. This aerogel consists of $Al_2O_3 \cdot H_2O$ strands with a characteristic diameter $\sim$50 nm and a characteristic separation of $\sim$200 nm (see Fig. 1 and the SEM-photo in [19]). The remarkable feature of this aerogel is that its strands are oriented along nearly the same direction at a macroscopic distance ($\sim$3–5 mm), i.e., this aerogel may be considered as almost infinitely stretched.

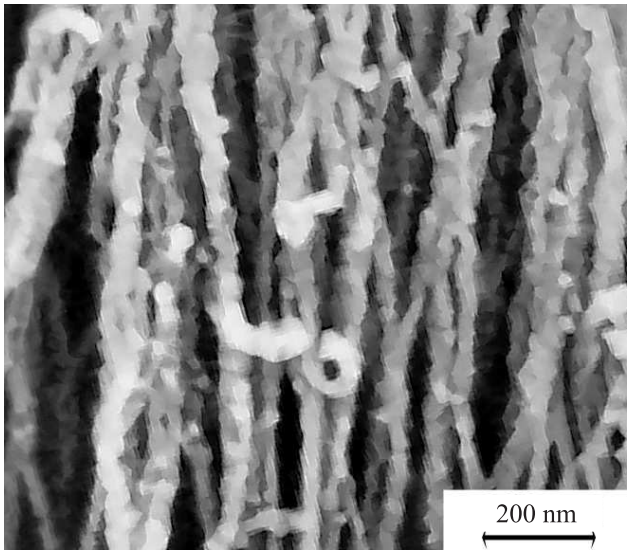

Fig. 1. The SEM-photo of "nematically ordered" aerogel

[1)] e-mail: dmitriev@kapitza.ras.ru

To emphasize this property we call it as "nematically ordered" aerogel.

2. Experimental setup. Our experimental chamber was made of epoxy resin Stycast-1266 and had two cylindric cells (see Fig. 2). Two aerogel samples with different porosities were placed freely in the cells. Samples had a form of a cylinder with the diameter ∼4 mm and with the heights 2.6 mm (the denser sample) and 3.2 mm (the less dense sample). Axes of the cylinders were oriented along aerogel strands ($\hat{\mathbf{z}}$-axis). Each cell was surrounded by transverse NMR-coil (not shown in Fig. 2) with the axis along $\hat{\mathbf{x}}$. Experiments were carried out in magnetic fields **H** from 106 up to 346 Oe (the range of NMR-frequencies was from 344 kHz up to 1.12 MHz) and at pressures from s.v.p. up to 29.3 bar. We were able to rotate **H** by any angle μ in the $\hat{\mathbf{y}}$–$\hat{\mathbf{z}}$-plane. Additional gradient coils were used to compensate an inhomogeneity of **H** and to apply the controlled field gradient. Residual inhomogeneity of **H** was $\sim 4 \cdot 10^{-5}$ for $\mu = 0$ and $\sim 4 \cdot 10^{-4}$ for $\mu = 90°$. About 30 % of the cell volumes were filled with the bulk liquid, but usually it was easy to distinguish the signal of superfluid ^{3}He in aerogel from bulk ^{3}He signal. Necessary temperatures were obtained by a nuclear demagnetization cryostat and were determined either by NMR in the A phase of bulk ^{3}He (when it was possible) or using a quartz tuning fork calibrated by measurements of the Leggett frequency in bulk ^{3}He-B. To avoid paramagnetic signal from solid ^{3}He aerogel samples have been preplated by ∼2.5 atomic monolayers of ^{4}He. The aerogel strands have bends and their surface is rough so we assume that, in spite of the preplating, a scattering of ^{3}He quasiparticles on the strands is diffusive.

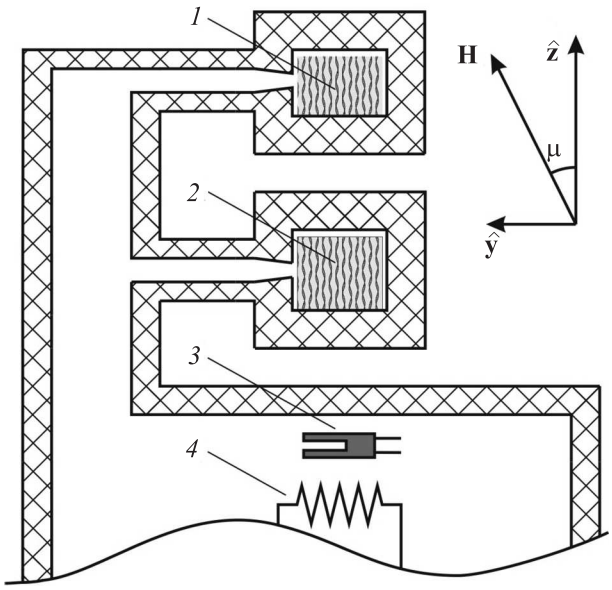

Fig. 2. The sketch of the experimental chamber: *1* – the denser sample; *2* – the less dense sample; *3* – quartz tuning fork; *4* – heater

The described setup has been used also for measurements of spin diffusion in normal liquid ^{3}He in the same aerogel samples [19]. The spin diffusion was found to be anisotropic in the limit of low temperatures. Quasiparticles effective mean free paths determined by aerogel strands were found to be: $\lambda_\parallel \approx 850$ nm, $\lambda_\perp \approx \approx 450$ nm (for the denser sample) and $\lambda_\parallel \approx 1600$ nm, $\lambda_\perp \approx 1100$ nm (for the less dense sample). Here $\lambda_\parallel$ and $\lambda_\perp$ are the mean free paths along and normal to the aerogel strands respectively.

Most of the experiments described below were done with the denser sample and the presented results were obtained using this sample if not specially mentioned.

3. Phase diagram. On cooling from the normal phase we observed a superfluid transition of ^{3}He in both aerogel samples. The transition was detected by continuous wave (CW) NMR with **H** parallel to the aerogel strands ($\mu = 0$): at the transition temperature (T_{ca}) a positive NMR-frequency shift ($\Delta\omega$) from the Larmor value appears. The transition temperature is suppressed in comparison with the superfluid transition temperature in bulk ^{3}He (T_c) and the suppression was found to be ∼2 times less in the less dense sample than in the denser sample. The pressure dependence of the suppression in terms of the superfluid coherence length ξ_0 is shown in Fig. 3.

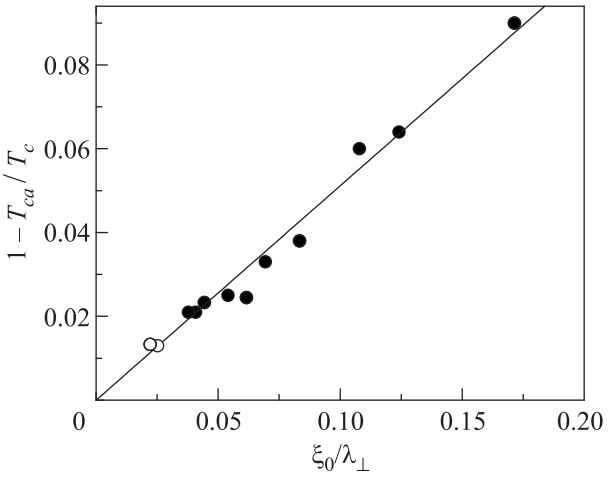

Fig. 3. The suppression of T_{ca} of ^{3}He in "nematically ordered" aerogel versus $\xi_0/\lambda_\perp$. ○ – the less dense sample, • – the denser sample. The line is the best fit by $y = Ax$ with $A = 0.51$

Fig. 4 shows the measured phase diagram of superfluid ^{3}He in "nematically ordered" aerogel. The filled

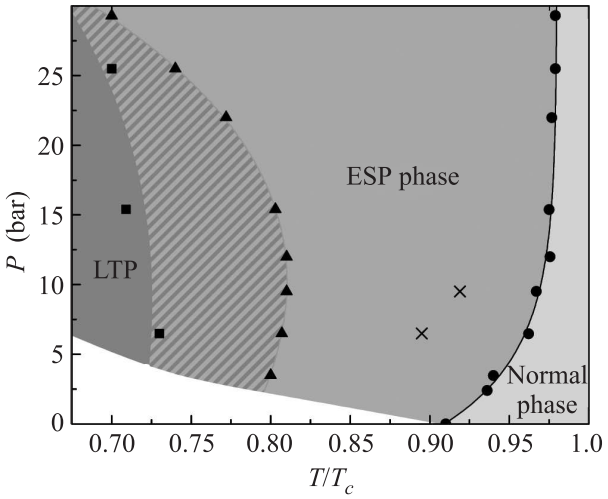

Fig. 4. The phase diagram of liquid ^{3}He in "nematically ordered" aerogel obtained on cooling from the normal phase. Note that the temperature is normalized to the superfluid transition temperature in bulk ^{3}He. See text for explanations

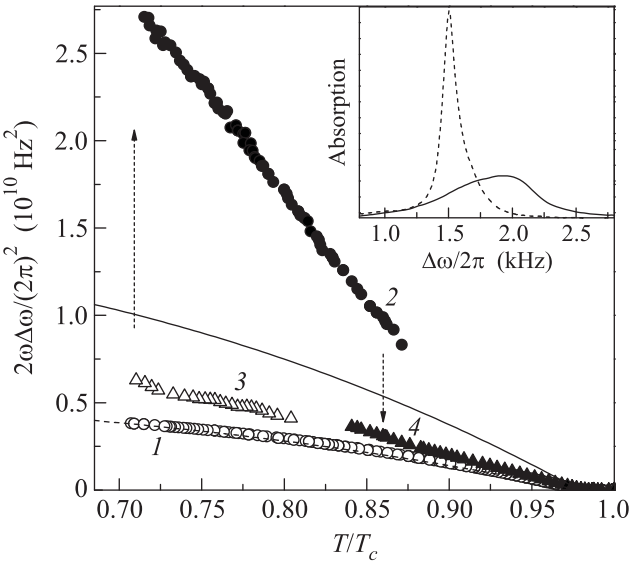

Fig. 5. The effective NMR-frequency shift versus temperature ($P = 29.3$ bar, $\mu = 0$, $T_{ca} = 0.979\,T_c$ and $H = 346$ Oe): *1* – the ESP1 phase; *2* – the LTP; *3* – the ESP2 phase on cooling; *4* – the ESP2 phase on warming. Solid and dashed lines (see Section 5 for the explanation). Insert: CW NMR-absorption lines in the ESP1 (dashed) and in the ESP2 phases (solid) at the same temperature ($T = 0.79\,T_c$)

circles correspond to the transition from the normal phase into a "high temperature" superfluid phase. This phase belongs to a family of Equal Spin Pairing (ESP) phases because its spin susceptibility is the same as in the normal phase and does not depend on T. Below we call this phase as the ESP1 phase. The triangles correspond to a beginning of the 1st-order phase transition from the ESP1 phase into a "low temperature" superfluid phase (LTP), where the susceptibility is less than in the normal phase. A region of coexistence of the LTP and the ESP1 phase is marked by a two-tone area fill. Such a coexistence may be due to a pinning of the interphase boundary on local inhomogeneities of the aerogel. The squares correspond to the end of the transition into the LTP. On subsequent warming the reverse 1st-order transition (from the LTP into the ESP phase) is clearly visible only at $P \geq 12$ bar and begins at higher temperatures ($\sim 0.85\,T/T_c$). More detailed description of the transitions and the superfluid phases is given below.

We have found that NMR-properties at high pressures ($P \geq 12$ bar) and at low pressures ($P \leq 6.5$ bar) are qualitatively different. The high pressure behavior is illustrated by Fig. 5 where we present the temperature dependence of the effective NMR-frequency shift ($2\omega\Delta\omega$, where ω is the NMR-frequency) in continuous wave (CW) NMR-experiments at $P = 29.3$ bar and with $\mathbf{H} \parallel \hat{\mathbf{z}}$. On cooling from the normal phase we observed the transition into the ESP1 phase with positive $\Delta\omega$ (open circles in Fig. 5). At $T \sim 0.7\,T_c$ the 1st-order transition into the LTP starts. The frequency shift in this phase is larger than in the ESP1 phase and on further cooling in some temperature range we observe two NMR-lines (from the LTP and from the ESP1 phase) with different values of $\Delta\omega$. After the complete transition, we observe on warming only the line from the LTP (filled circles in Fig. 5) until the reverse transition starts ($\sim 0.84\,T/T_c$). Surprisingly, the obtained in a such way the ESP phase (we call it as ESP2 phase) is different from the ESP1 phase: it has larger $\Delta\omega$ up to T_{ca} (filled triangles in Fig. 5) and larger the NMR linewidth (insert of Fig. 5). Being obtained, this ESP2 phase remains stable down to $T \sim 0.7\,T_c$ (open triangles in Fig.5).

Fig. 6 shows an example of the low pressure behavior. Here the dependence of $2\omega\Delta\omega$ on T at $P = 6.5$ bar is presented. On cooling from the normal phase we get the ESP1 phase (open circles in Fig. 6). Then, at $T \sim 0.8\,T_c$, the transition into the LTP begins. This transition completes at $\sim 0.73\,T_c$ and on subsequent warming the LTP smoothly transforms into the ESP phase (filled circles in Fig. 6). This smooth transition ends at $T_x = T \sim 0.91\,T_c$: above this temperature $\Delta\omega$ and the linewidth are the same as in the ESP1 phase.

At intermediate pressures (6.5 bar$< P <$ 12 bar) we can not distinguish between these two types of the behavior: no jump of $\Delta\omega$ is seen, but the absolute value of the slope of the dependence $\Delta\omega = \Delta\omega(T)$ essentially increases just below T_x. At these pressures and near T_x

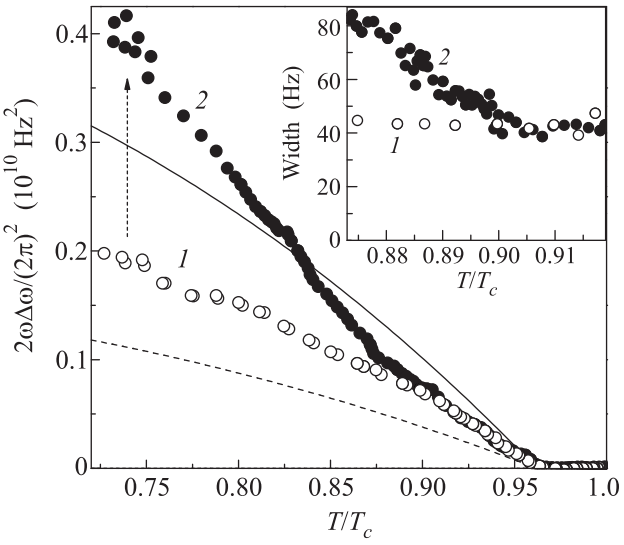

Fig. 6. The effective NMR-frequency shift versus temperature ($P = 6.5$ bar, $\mu = 0$, $T_{ca} = 0.962\,T_c$, and $H = 346$ Oe: *1* – the ESP1 phase; *2* – the LTP. Solid and dashed lines (see Section 5 for the explanation). Insert: corresponding CW NMR-linewidths

the NMR-frequency shifts in the LTP and ESP phases are close to each other, so the final temperature width of the transition may mask a jump of $\Delta\omega$. It is also possible that inhomogeneities in the aerogel result in different types of the transition at different places of the sample.

4. Low temperature phase. At high pressures the transition from the ESP phase into the LTP is accompanied by a sharp decrease of the spin susceptibility and, on further cooling, the susceptibility is decreasing. For $\mathbf{H} \parallel \hat{\mathbf{z}}$ the NMR-frequency shift in the LTP is a few times larger than in the ESP phase and is close to the value expected for bulk ^{3}He-B with $\hat{\mathbf{l}} \perp \mathbf{H}$, where $\hat{\mathbf{l}}$ is an orbital vector oriented along the direction of the gap anisotropy [20]. For example, at 29.3 bar and at $T = 0.75\,T_{ca}$ the ratio of the observed shift and of the expected bulk B phase shift is 0.86. Correspondingly, we assume that at high pressures the order parameter of the LTP is close to the parameter of bulk ^{3}He-B and aerogel strands orient $\hat{\mathbf{l}}$ normal to $\hat{\mathbf{z}}$.

At low pressures the LTP is not so close to bulk ^{3}He-B. Firstly, with decreasing pressure the above-mentioned ratio decreases down to 0.4 at $P = 3.5$ bar. Secondly, the susceptibility hardly changes during the transition from the ESP1 phase into the LTP.

The properties of the LTP may be explained if we suggest that the order parameter corresponds to the order parameter of bulk ^{3}He-B with the polar distortion. Aerogel strands suppress the gap in directions normal to their axes, i.e. normal to $\hat{\mathbf{z}}$. If we choose the direction $\hat{\mathbf{l}}$ along $\hat{\mathbf{x}}$, then the distorted B phase order parameter matrix averaged over distances much larger than ξ is:

$$\mathbf{A} = \mathbf{R}\begin{pmatrix} b & 0 & 0 \\ 0 & b & 0 \\ 0 & 0 & a \end{pmatrix} = \begin{pmatrix} 0 & 0 & aR_{13} \\ bR_{21} & bR_{22} & 0 \\ bR_{31} & bR_{32} & 0 \end{pmatrix}, \quad (1)$$

where $\mathbf{R} = \mathbf{R}(\mathbf{n}, \Theta)$ is pure B phase order parameter rotation matrix, a and b are positive and $a^2 + 2b^2 = 1$. If $a = b$ then we get pure Balian–Werthamer (BW) state with isotropic energy gap (the case of bulk ^{3}He-B in weak magnetic field). Note that $b/a = \Delta_\perp/\Delta_\parallel < 1$, where $\Delta_\perp$ and $\Delta_\parallel$ are values of the gap in directions normal and along $\hat{\mathbf{z}}$ respectively. The limit $a = 1$ and $b = 0$ corresponds to the polar phase. The observed temperature dependencies of $\Delta\omega$ show that a and b depend on temperature and pressure: the ratio b/a is larger at lower temperatures and at higher pressures.

5. ESP phases. Following [16] we can suggest three variants for the ESP phase: 1) it can be analog of the A phase, i.e. its order parameter corresponds to Anderson–Brinkman–Morel (ABM) model; 2) it can be the A phase with the polar distortion; 3) it can be the polar phase. The energy gap should be maximal along $\hat{\mathbf{z}}$ and minimal in the $\hat{\mathbf{x}}$–$\hat{\mathbf{y}}$-plane. If we choose $\hat{\mathbf{x}}$ as a direction along which the gap is minimal then a general form of the order parameter matrix for all three cases is:

$$\mathbf{A} = \begin{pmatrix} 0 & ib & a \\ 0 & 0 & 0 \\ 0 & 0 & 0 \end{pmatrix}, \quad (2)$$

where a and b are positive and $a^2 + b^2 = 1$. Here we suggest that the angle between $\hat{\mathbf{x}}$ and spin vector $\hat{\mathbf{d}}$ is zero. The pure ABM phase corresponds to $a = b$, while for the pure polar phase $a = 1$ and $b = 0$.

We have carried out additional NMR-experiments with ESP1 and ESP2 phases. In CW NMR-experiments the dependence of $\Delta\omega$ on μ was measured. In the denser sample we have found that $\Delta\omega$ is positive for $\mu = 0$ and equals zero for $\mu = 90°$. In the less dense sample measurements have been done also for $\mu = 16°$ and for $\mu = 33°$ and it was found that $\Delta\omega \propto \cos^2\mu$. In pulsed NMR-experiments the dependence of the initial frequency of a free induction decay signal (FIDS) on the tipping angle of the magnetization (β) was measured. It was found that $\Delta\omega \propto \cos\beta$ for $\mathbf{H} \parallel \hat{\mathbf{z}}$ and $\Delta\omega \propto (1 - \cos\beta)$ for $\mathbf{H} \perp \hat{\mathbf{z}}$ (see Fig. 7). These results definitely exclude the spatially homogeneous ABM (or distorted ABM) order parameter for both ESP1 and

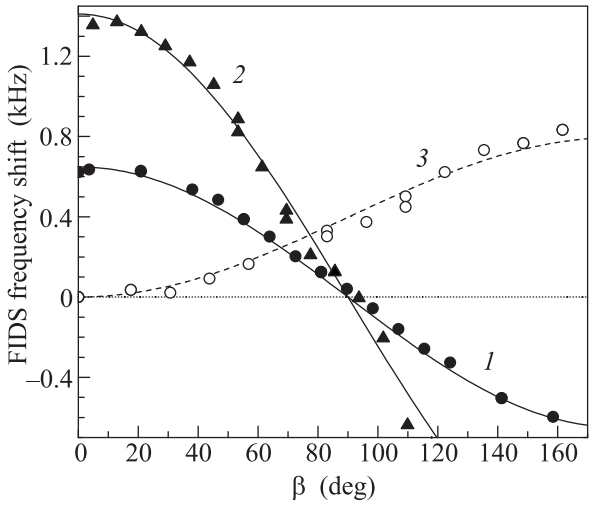

Fig. 7. The initial frequency of the FIDS versus β: *1* – the ESP1 phase, $\mu = 0, P = 9.5$ bar, $T = 0.85\,T_c$, $H = 346$ Oe; *2* – the ESP2 phase, $\mu = 0, P = 29.3$ bar, $T = 0.835\,T_c$, $H = 346$ Oe; *3* – the ESP1 phase, $\mu = 90°, P = 12$ bar, $T = 0.87\,T_c$, $H = 106$ Oe. Solid lines and the dashed line are the best fits by $\cos\beta$ and $1 - \cos\beta$ dependencies respectively

ESP2 phases but qualitatively agree with an equation for $\Delta\omega$ for the polar phase [16]:

$$2\omega\Delta\omega = C\left(\cos\beta - \sin^2\mu\frac{5\cos\beta - 1}{4}\right), \qquad (3)$$

where $C = \Omega_p^2$ and Ω_p is the Leggett frequency for the polar phase. However, we should consider also another possibility: our aerogel can be considered as almost infinitely stretched and the ABM order parameter (as well as the distorted ABM order parameter) can be in a two dimensional Larkin–Imry–Ma (LIM) state. This state corresponds to a spatially inhomogeneous distribution of $\hat{\mathbf{l}}$ in the $\hat{\mathbf{x}}$–$\hat{\mathbf{y}}$ plane [13, 15]. A characteristic length of these inhomogeneities should be less than the dipole length, because well below T_{ca} the observed CW NMR-linewidths are small in comparison with $\Delta\omega$. For the ABM phase in the LIM state the dependence of $\Delta\omega$ on μ and β is also given by (3) (see Eq. (15) in [13]) but with different C. For a general case C can be calculated in weak coupling limit:

$$C = 2\Omega_A^2\frac{3a^2 - 1}{3 - 4a^2b^2}, \qquad (4)$$

where Ω_A is the Leggett frequency in the pure ABM phase. For $a = b = 1/\sqrt{2}$ (the ABM phase in the LIM state) $C = \Omega_A^2/2$, while for $a = 1$, $b = 0$ (the polar phase) $C = 4\Omega_A^2/3 = \Omega_p^2$.

Thus, our results indicate that ESP phases have the order parameter (2) and, depending on a and b, may correspond either to the polar or to the LIM state of the ABM phase with the polar distortion. ESP1 and ESP2 phases can exist at the same conditions and presumably have different values of a and b. The value of $\Delta\omega$ allows, in principal, to find C and to calculate a and b: if $\mu = 0$ and $\beta = 0$, then $C = 2\omega\Delta\omega$. The problem is that Ω_A for ^{3}He in our aerogel is unknown. Therefore, in the first approximation, we have used data for Ω_A in bulk ^{3}He-A [21–23] rescaled in assumption that the relative suppression of Ω_A equals the relative suppression of the superfluid transition temperature (T_{ca}/T_c). Using these values of Ω_A the expected dependencies of $2\omega\Delta\omega$ on temperature for the pure polar phase and for the pure ABM phase in the LIM state have been calculated (dashed and solid lines respectively in Figs. 5 and 6). It is seen that at 29.3 bar the ESP1 phase is close to the pure ABM phase in the LIM state while at 6.5 bar the polar distortion is essential.

6. Search for pure polar phase. The polar distortion of the ABM order parameter depends on temperature and is expected to be larger near T_{ca} [16]. To characterize this distortion we introduce a parameter $K = C/\Omega_A^2$ and denote its value in the limit $T \to T_{ca}$ as K_0. For the pure ABM phase in the LIM state K should be equal to 0.5 while for the pure polar phase we expect $K = 4/3$. The experimental dependence of K_0 on pressure is shown in Fig. 8. At low pressures

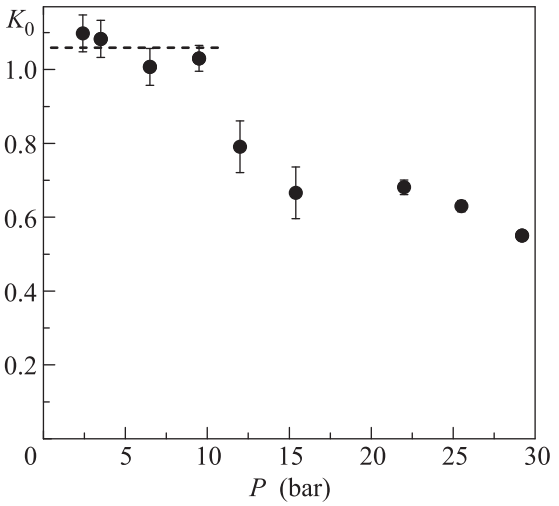

Fig. 8. The dependence of K_0 on pressure

$K_0 \approx 1.07$ (dashed line in Fig. 8) and from (4) we find that it corresponds to a strongly distorted ABM phase with $a^2 = 0.73$ and $b^2 = 0.27$. However, we can not exclude that the pure polar can be realized at low pressures near T_{ca}. The point is that the suppression of the bulk value of Ω_A may be larger than we have used in our estimation of C as it happens in the case of ^{3}He in

standard silica aerogel [24, 25] or as it follows from a slab model [26]. In fact at $P < 12$ bar an additional suppression of Ω_A^2 by 25 % is enough to get $K = 4/3$. One more argument in favor of the polar phase is that at low pressures $K \geq 1$ in a finite range of temperatures below T_{ca} and starts to decrease on further cooling below some temperature $T_k < T_{ca}$. The values of T_k at 6.5 and 9.5 bar are shown by crosses in Fig. 4. At 2.4 and 3.5 bar the decrease of K have not been observed till the lowest obtained temperatures. We note also that at low pressures the transition from the LTP into the ESP1 phase is continuous. This is possible if the distorted BW phase transforms into the polar phase (see Eq. (1) with $b \to 0$), while the transition into the ABM (or into the distorted ABM) phase should be of the 1st-order as we observe at high pressures.

7. Conclusions. We have measured the phase diagram of superfluid phases of ^{3}He in "nematically ordered" aerogel. Depending on conditions and the prehistory 3 superfluid phases were observed: the LTP, the ESP1 phase, and the ESP2 phase. The LTP presumably has BW order parameter with the polar distortion, while the ESP1 and the ESP2 phases correspond to the ABM order parameter with different values of the polar distortion. There are indications that at low pressures the pure polar phase may exist in some range of temperatures just below T_{ca}. However, additional experiments are necessary to check such a possibility.

Existing theoretical models for superfluid ^{3}He in aerogel or for the case of restricted geometry cannot be directly applied to our case. Inhomogeneous isotropic scattering model [24] which well describes ^{3}He in nearly isotropic silica aerogel, considers the isotropic scattering of quasiparticles and surely can not be used to interpret our results. The theoretical model of K. Aoyama and R. Ikeda [16] of the A-like phase in stretched aerogel is much closer to our situation and our results for ESP phases qualitatively do not contradict this model. However, the case of a strong anisotropy of the quasiparticles mean free path has not been considered in [16]. We also note that the B phase with polar-type distortion has been theoretically considered in detail only for the case of ^{3}He inside narrow cylindrical channels. Correspondingly, we think that further theoretical investigations are necessary to explain the observed properties of superfluid ^{3}He in "nematically ordered" aerogel.

We thank I.A. Fomin, W.P. Halperin, E.V. Surovtsev, and G.E. Volovik for useful discussions. This work was supported in part by the Russian Foundation for Basic Research (grants # 11-02-12069, 09-02-01185) and by the Ministry of Education and Science of Russia (contract # 16.513.11.3036).

1. V. Ambegaokar, P. G. de Gennes, and D. Reiner, Phys. Rev. A **9**, 2676 (1974).
2. G. Barton and M.A. Moore, J. of Low Temp. Phys. **21**, 75 (1975).
3. Y. H. Li and T. N. Ho, Phys. Rev. B **38**, 2362 (1988).
4. L. V. Levitin, R. C. Benett, A. J. Casey et al., J. of Low Temp. Phys. **158**, 159 (2010).
5. L. V. Levitin, Ph.D. thesis, Royal Holloway, University of London, 2010.
6. V. Kotsubo, K. D. Hahn, and J. M. Parpia, Phys. Rev. Lett. **58**, 804 (1987).
7. J. P. Pekola, J. C. Davis, Z. Yu-Qun et al., J. of Low Temp. Phys. **67**, 47 (1987).
8. J. V. Porto and J. M. Parpia, Phys. Rev. Lett. **74**, 4667 (1995).
9. D. T. Sprague, T. M. Haard, J. B. Kycia et al., Phys. Rev. Lett. **75**, 661 (1995).
10. B. I. Barker, Y. Lee, L. Polukhina et al., Phys. Rev. Lett. **85**, 2148 (2000).
11. V. V. Dmitriev, V. V. Zavjalov, I. V. Kosarev et al., Pis'ma v ZhETF **76**, 371 (2002) [JETP Lett. **76**, 321 (2002)].
12. T. Kunimatsu, T. Sato, K. Izumina et al., Pis'ma v ZhETF **86**, 244 (2007) [JETP Lett. **86**, 216 (2007)].
13. V. V. Dmitriev, D. A. Krasnikhin, N. Mulders et al., Pis'ma v ZhETF **91**, 669 (2010) [JETP Lett. **91**, 599 (2010)].
14. J. Pollanen, J. I. A. Li, C. A. Collett et al., Phys. Rev. Lett. **107**, 195301 (2011).
15. G. E. Volovik, J. of Low Temp. Phys. **150**, 453 (2008).
16. K. Aoyama and R. Ikeda, Phys. Rev. B **73**, 060504 (2006).
17. J. Pollanen, K. R. Shirer, S. Blinstein et al., J. Non-Cristallin Solids **354**, 4668 (2008).
18. R. Sh. Askhadullin, P. N. Martynov, P. A. Yudintsev et al., J. Phys.: Conf. Ser. **98**, 072012 (2008).
19. R. Sh. Askhadullin, V. V. Dmitriev, D. A. Krasnikhin et al., J. Phys.: Conf. Ser. (to be published, 2nd Quarter 2012).
20. M. M. Salomaa and G. E. Volovik, Rev. Mod. Phys. **59**, 533 (1987).
21. P. E. Schiffer, Ph.D. thesis, Stanford University, 1993.
22. A. I. Ahonen, M. Krusius, and M.A. Paalanen, J. of Low Temp. Phys. **25**, 421 (1976).
23. M. R. Rand, H. H. Hensley, J. B. Kycia et al., Physica B **194–196**, 805 (1994).
24. E. V. Thuneberg, S. K. Yip, M. Fogelstrom, and J. A. Sauls, Phys. Rev. Lett. **80**, 2861 (1998).
25. W. P. Halperin, H. Choi, J. P. Davis, and J. Pollanen, J. of Phys. Soc. of Japan **77**, 111002 (2008).
26. E. V. Thuneberg, M. Fogelstrom, S. K. Yip, and J. A. Sauls, Czech. J. Phys. **46**, 113 (1996).